International Journal of Heat and Mass Transfer 124 (2018) 124–130

Contents lists available at ScienceDirect

International Journal of Heat and Mass Transfer

journal homepage: www.elsevier.com/locate/ijhmt

Numerical and experimental investigation on thermal shock failure of Y_2O_3-coated CVD ZnS infrared windows

Xing Liu, Jiaqi Zhu *, Jiecai Han

Center for Composite Materials and Structures, School of Astronautics, Harbin Institute of Technology, Harbin 150001, China

ARTICLE INFO

Article history:
Received 23 October 2017
Received in revised form 17 February 2018
Accepted 18 March 2018

Keywords:
Infrared window
CVD ZnS
Yttrium oxide
Thermal shock
Oxygen–propane flame
Finite element analysis

ABSTRACT

Infrared transparent windows on aircraft and missiles can be subjected to extreme aerothermodynamics, which can cause thermal shock failure. Finite element analysis and oxygen–propane flame jet impingement tests were performed to investigate the thermal shock failure of an yttrium oxide-coated chemical vapor deposition (CVD) ZnS infrared window. Good agreement was achieved between the simulation and experimental results, which indicated that thermal shock failure occurs under high temperature differences and thermal stresses. The temperature and stress in the samples increased rapidly in a few seconds and then trended to be stable. The center area of the window surface failed most easily because the maximum temperature and stress both occurred in this area. No delamination of the Y_2O_3 films occurred during the thermal shock, which indicated good adhesion between the Y_2O_3 films and CVD ZnS substrate. In the experiment, the center area of the specimen surface was damaged in the form of pits and line cracks.

1. Introduction

The infrared transparent window is one of the most important components for an aircraft guidance system [1]. It is subjected to extreme aerodynamic friction and heating when a high-Mach vehicle accelerates from launch [2–5]. High temperatures and large temperature gradients are caused by the localized heating [6,7]. These temperature gradients can result in sufficient thermal expansion stress to cause component failure [8–10]. Investigating the thermal shock failure of infrared transparent windows will contribute to improving their design.

The development of infrared optical materials is closely related to the research and exploration of materials science [11,12]. Chemical vapor deposition (CVD) ZnS and sapphire are widely used as substrate materials for infrared windows because of their high transmittance and perfect mechanical properties [2,13,14]. The function of the infrared window is improved by employing antireflective and protective films, such as diamond-like carbon (DLC) [15,16], yttrium oxide (Y_2O_3) [17,18], germanium carbide ($Ge_{1-x}C_x$) [19,20], zirconium nitride (ZrN) [21], yttrium fluoride (YF_3) [22], and boron phosphide (BP) [23].

Experiments and numerical simulation are two methods for investigating the thermal shock failure of infrared windows. The main experimental schemes to achieve thermal shocking include hardening, flame striking [24,25], wind tunnels [26], and laser shocking [27]. Hingst and Korber [28] carried out a series of wind-tunnel tests focused on the thermal shock behavior of different infrared window shapes under critical flight conditions. Russell et al. [29] used the ATAC3D aerothermal analysis code to provide convective and pressure boundary conditions, which they coupled with the ANSYS finite element analysis code to solve the three-dimensional finite element problem for analyzing the thermal shock of infrared windows. They also conducted aerothermal testing at the Naval Air Warfare Center T-Range Aerothermal Test Facility and ultimately performed flight tests at Eglin Air Force Base to validate their analysis. Because thermal shock testing is expensive, and some data are difficult to measure, so numerical simulations are a good way to validate and predict the performance of infrared windows. Cheng et al. [30] experimentally investigated the flexural properties of CVD ZnS from room temperature to 1050 °C and expounded the mechanisms for its mechanical behavior. Peng et al. [31] experimentally investigated the laser-induced thermal–mechanical damage characteristics of infrared window materials and concluded that the damage originates from the thermal stress but not the melting. Zimmermann et al. [32] used finite element analysis to estimate the temperatures and stresses on infrared window materials. Cho and Kardomateas [33] developed an elastodynamic solution for thermal shock due to heat convection at a constant temperature in a thick orthotropic cylindrical shell and presented the complete dynamic response of thermal shock stresses. Cheng et al. [34] measured the compressive and

* Corresponding author.
E-mail address: zhujiaqi@hit234.com (J. Zhu).

https://doi.org/10.1016/j.ijheatmasstransfer.2018.03.062
0017-9310/

tensile strengths of CVD ZnS from room temperature to 600 °C and found that the thermal shock resistance of CVD ZnS under aerodynamic thermal environments will be over estimated if the compressive strength is neglected. Liu et al. [35,36] studied the structural and thermal radiation properties of yttrium oxide sputtered on sapphire and the thermal responses indicated that the Y_2O_3 could apparently reduce the maximum temperature in the window. Qu et al. [37] numerically and experimentally studied the thermal shock failure of CVD ZnS infrared window by the finite element analysis and rapid heating thermal shock experiments. The results showed that the critical failure temperature difference for thermal shock failure was ~375 °C.

However, there has been less experimental and numerical research on thermal shock damage to CVD ZnS/Y_2O_3 infrared systems. In this study, a finite element model was developed to simulate the temperature and stress distributions in an infrared window (CVD ZnS/Y_2O_3). Additionally, an oxygen–propane flame jet impingement test was performed to investigate the thermal shock failure of the infrared window. The temperature changes over time were measured, and microscope images were taken to evaluate the damage to the infrared window.

2. Models

2.1. Thermal and stress model

For a cylindrical specimen, the temperature of the system can be described as follows:

$$\rho c_p \frac{\partial T}{\partial t} = k\left[\frac{\partial^2 T}{\partial y^2} + \frac{\partial^2 T}{\partial r^2} + \frac{1}{r}\frac{\partial T}{\partial t}\right] \quad (1)$$

where ρ is the solid density (kg/m^3), c_p is the solid specific heat (kJ/(kg K)), T is the system temperature (K), t is the time (s), and k is the solid thermal conductivity (W/(m K)).

The third boundary condition applied to this model is expressed as

$$-k\frac{\partial T}{\partial n}\bigg|_{\tau_c} = h(T_w - T_f) \quad (2)$$

where $\partial T/\partial n$ is the normal temperature gradient (K/m), τ_c is the time constant (s), h is the heat transfer coefficient (W/(m^2 K)), T_f is the ambient temperature (K), and T_w is the temperature of the specimen (K).

The stress and strain must satisfy the following equations:

Balance equation

$$\left.\begin{aligned} \frac{\partial \sigma_r}{\partial r} + \frac{\partial \tau_{zr}}{\partial y} + \frac{\sigma_r - \sigma_\theta}{r} + f_r = 0 \\ \frac{\partial \tau_{ry}}{\partial r} + \frac{\partial \sigma_y}{\partial y} + \frac{\tau_{rz}}{r} + f_y = 0 \end{aligned}\right\} \quad (3)$$

Physical equation:

$$\begin{Bmatrix} \sigma_r \\ \sigma_\theta \\ \sigma_y \\ \tau_{ry} \end{Bmatrix} = \frac{E(1-\mu)}{(1+\mu)(1-2\mu)}\begin{bmatrix} 1 & A_1 & A_1 & 0 \\ A_1 & 1 & A_1 & 0 \\ A_1 & A_1 & 1 & 0 \\ 0 & 0 & 0 & A_2 \end{bmatrix}\begin{bmatrix} \varepsilon_r - (1+\mu)\alpha\Delta T \\ \varepsilon_\theta - (1+\mu)\alpha\Delta T \\ \varepsilon_y - (1+\mu)\alpha\Delta T \\ \gamma_{ry} \end{bmatrix} \quad (4)$$

where σ is the normal stress (Pa), τ is the shearing stress (Pa), f is the component of the body force (N/m^3), ε is the linear strain (m), γ is the shear strain (m), E is the Young's modulus (MPa), μ is Poisson's ratio, α is the thermal expansion coefficient (1/K), ΔT is the increment of temperature (K), $A_1 = \mu/(1-\mu)$, and $A_2 = (1-2\mu)/[2(1-\mu)]$.

2.2. Physical and mesh model

Because the test sample was a cylindrical CVD ZnS substrate coated with an Y_2O_3 thin film on the surface and had axial symmetry, a 2D axisymmetric model was used to simulate the problems. Fig. 1 shows the model, and Table 1 lists the structural dimensions of the test sample. The sample diameter and thickness were 30.0 mm and 8.0 mm, respectively, and the film thickness was 1.0×10^{-3} mm. Table 2 lists the mechanical and thermo-physical properties of CVD ZnS and Y_2O_3.

A finite element analysis method was applied to investigate the thermal and stress distributions of the infrared window. ANSYS®14.0 was used in this work with the Plane 13 element. In order to simulate the temperature and stress more accurately, the grids were refined at the connection of the film and substrate, as shown in Fig. 2. A dense grid scheme was used in the model. The total number of the elements is 3900, including 300 elements in the film and 3600 elements in the substrate.

2.3. Boundary conditions

Because the thermal shock test is an impinging jet system, pronounced variations in the air flow beyond the impinging zone are expected. To consider a uniform coefficient in the jet radius region and flow attenuation beyond it, a simplified model was used to simulate the radial variation of the heat transfer coefficient [38].

Table 1
Structural dimensions of the test sample.

Symbol	Diameter (mm)	Thickness of the substrate (mm)	Thickness of the film (mm)
Value	30.0	8.0	1.0×10^{-3}

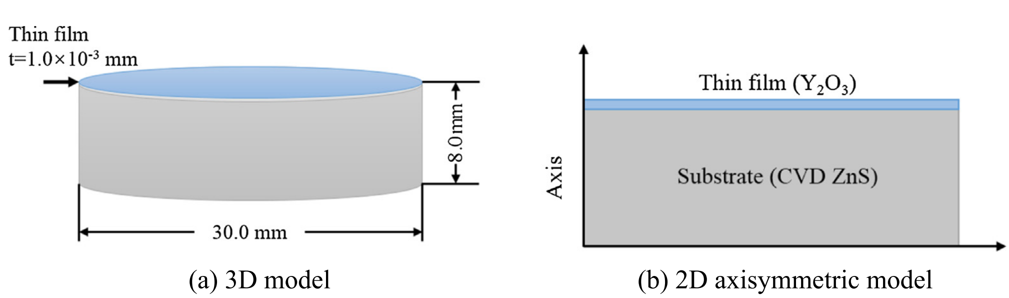

Fig. 1. Simulation model and structural dimensions of the window (mm).